

Research on Shape Perception of the Soft Gripper Based on Triboelectric Nanogenerator

Long Li, Tianhong Wang, Tao Jin, Peifeng Ma, Yichen Jiang, Guangjie Yuan, Yingzhong Tian*

Abstract - Soft robotics is an exciting novel research field and has great potentiality in human-machine cooperation. This kind of robot can undergo large deformations to execute complex motions, which leads to the difficulty to apply traditional sensors and the lack of necessary feedback. Therefore, we want to create a sensory finger that is able to grasp and hold heavy objects. This work explores the potential of triboelectric nanogenerators (TENGs) and presents the demonstration of TENG based on tactile sensors integrated into the structure of a soft finger with variable stiffness. For displaying the sensing result, three soft fingers were assembled to form a soft gripper. Our result shows that the tactile sensor with strip electrodes can detect the contact position when comparing the output difference in different electrodes. In order to describe the shape of the grab target, in this paper, we theoretically analyze the relative position relationship of the end before and after the finger bending deformation, and obtain the finger-bending mode. In the demonstration, the gripper integrating with the sensor can roughly distinguish the scale of the object by combining tactile perception capability. The proposed highly pliable fingers can help the robot handle the fragile and soft objects and appropriately recognize their shapes in complex environment.

Index Terms - Soft robotics, soft gripper, grasping, triboelectric nanogenerator, tactile sensor.

I. INTRODUCTION

Soft robotics has become one of the hotspots in robotic research in order to tackle challenges faced by traditional robots. They are usually consisted of super-elastic, soft materials or a combination, leading to the robots performing high compliance and dispelling the safety concerns in human-robot cooperation [1–5]. Herein, this kind of technology has attracted tremendous attention in recent years. However, the large nonlinear deformation and no joint structure also hinder the application of traditional sensing devices like potentiometer and encoders. Due to the limitation of sensors, the main control method still depends on kinematics [4, 6] or dynamics [7, 8] of the soft robots, which always lacks of the feedback. So it is necessary to develop sensing method displaying both flexibility and small extra load for the closed-loop control of soft robotics.

*Research supported by National Natural Science Foundation of China (U1637207, 61673287) and National Science Foundation for Young Scientists of China (51705098).

Long Li, Tianhong Wang, Tao Jin, Peifeng Ma, Yichen Jiang, Guangjie Yuan, and Yingzhong Tian are with School of Mechatronic Engineering and Automation, Shanghai University, Shanghai Key Laboratory of Intelligent Manufacturing and Robotics, Shanghai, 200444, China. (Yingzhong Tian is the corresponding author, troytian@shu.edu.cn)

Till now, some solutions, which usually use external camera [9], smart material [10], magnetic sensor [11] or optic fibre [12], have been come up to achieve the motion perception of soft robotics. However, these solutions still have some problems. For external camera methods, the camera is hard to adapt to the invisible environment. The sensors based on smart material and optic fiber require calibration as the output will change in different length and width. Besides, the requirement of magnetic field confines the magnetic sensor to be used in some limited situation. At the same time, the triboelectric nanogenerators (TENGs) based on triboelectrification and electrostatic induction display incredible potentiality in multifunction self-power sensing with ultra-high output and simple structure since first reported in 2012 [13–15]. The output depend on the stimulus and the electronegativity difference of various materials [16–18]. To our best knowledge, this powerful technology has been successfully applied into human-robot interaction [18, 19]. Due to the diversity of the flexible material, the sensor based on TENG technology also can be compatible with the soft robotics [20].

As 3D printing technology is applicable to the production of various complex shapes, with high accuracy and low processing cost, previous researchers, enthusiasts and teachers are enthusiasm to adapt such approach to carry out the researches on flexible finger. In this paper, we proposed a soft gripper integrating with tactile sensors according to TENG mechanism, and complete the following contribution: Firstly, a sealed pneumatic soft finger with variable stiffness and good robustness was manufactured by 3D printing technology. Secondly, we analyzed the geometric relationship of flexible deformation of bellows in soft fingers to theoretically characterize the bending capability of the soft finger. Thirdly, the tactile sensor was tested for comparing the output difference when the contacting position changed. Finally, the sensors were integrated into the soft gripper and then the gripper was used to grip and distinguish various scale objects.

II. DESIGN AND MANUFACTURE METHODS

A. Soft Gripper Manufacture

A variety of research group have developed several categories of soft fingers for gripper, gloves, prosthetics etc [12, 21, 22]. However, universal robotic fingers integrating varieties of sensors usually have the properties of high precision control and stiffness, but the complex feedback system. When it comes to human-robot interaction, safety inevitably become the focus of all attentions[23, 24]. The aim of this work is to design a soft pneumatic finger with high compliance, which can effectively sense the shape and size of the grasping target by applying sensor based on TENG technology. Hence, it is a crucial point to fabricate a flexible finger with variable stiffness. Here the

bellows-type was considered as actuator. In view of some previous works on related robotics, most actuators were driven by air to make the flexible cavity expand and bend. By setting diverse wall thickness in different directions, the soft robot can move in a certain way, even by setting stiffness enhancement at joints in order to realize continuous bending like a human hand. As depicted in Fig.1, due to the good forming property, TPU (Thermoplastic Urethane) is an ideal material for soft structures because of its outstanding flexibility. It can be fused at high temperature and polymerized after cooling. Moreover, the Young's modulus of TPU filament is approximately 2×10^7 Pa. Therefore, we use this characteristic to fabricate air-tight structures (see Fig1, a). The soft finger of our work is directly actuated by bellows, and high-pressure air is injected into one end of the finger. The air path between each driver is connected. Due to good elasticity and elongation of TPU, high-pressure air will lead to the drive expansion and deformation, extrusion stress between two adjacent drivers. Therefore, the movement of the soft finger is driven by continuous contact force.

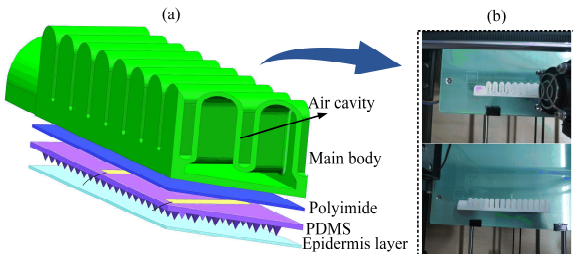


Fig.1 (a) The structure of the soft gripper integrated with TENG-based tactile sensor.(b) the process of the actuator being printed using 3D printer.

The structure of soft finger is design in SOLIDWORKS, a 3D computer-aid-designed software. It consists of a sealing surface and a air channel (Fig2). The air tap is inserted into the channel, which allows the soft finger to be connectd to external air source. Air tightness of the actuator is the key to enable finger move, a few rules should to be followed when printing: (1) Extruder temperature should not be too low, which would bring about the air leakage due to tiny gaps caused by incomplete melting. (2)As the filament strands are circle, the layer height should be small enough set in software, which can further reduce the possibility of air leakage due to improper

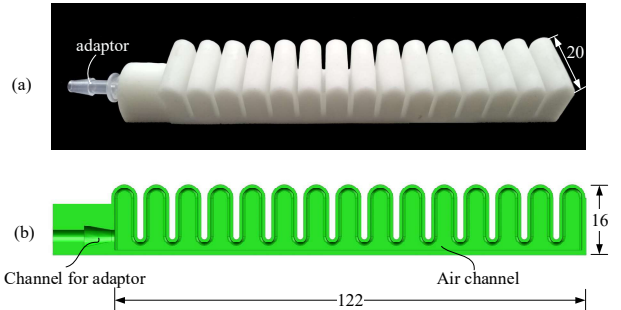


Fig.2 (a) Photograph of the printed soft finger with an air tap that will be connected to the air source. (b) 2D sectional drawing to show the inner structure.

fuse. (3) Ensure that the nozzle and platform are clean to prevent the introduction of impurities, such as old material may stick, resulting in actuator clearance.(4) In order to ensure that the actuator can withstand greater pressure and reduce the layer gap, the transverse or longitudinal printing is suggest to replaced by staggered printing, which is beneficial to increase the strength and air tightness of air cavity. (5) To improve the success ratio, it is highly suggested that the flank should be laid flat on the platform, which can efficiently decrease the possibility of printing without support.

B. The Tactile Sensor Based on TENG (T-TENG)

The TENG technology can be used to detect the press so that it has the potential to play as a tactile sensor. As shown in Fig3. b, the basic working principle of T-TENG sensor is based on triboelectrification and electrostatic induction. It is easy to understand that the object with the evenly distributed charge will output high voltages as the contacting area enlarges. The details structure can be seen in Fig.3a, where the Cu bar is coating on the polydimethylsiloxane (PDMS) substrate and the Cu bar is wrapped by the negative friction material silicone rubber (ecoflex-0030, Smooth on). Initially, no pressure is applied to the device, and the upper silicone layer and the lower aluminum layer are separated by triangular stripes. When applied with external force, triboelectrification occurs because of relative movement between the triangle stripe and the lower aluminum electrode. Due to the strong oxidation in chemistry, the Al electrode generates the positive charges. To balance the potential, the same amount of negative charges also appear in the PDMS pole, as shown in the Fig.3b. With the two poles approach to each other, the contact area

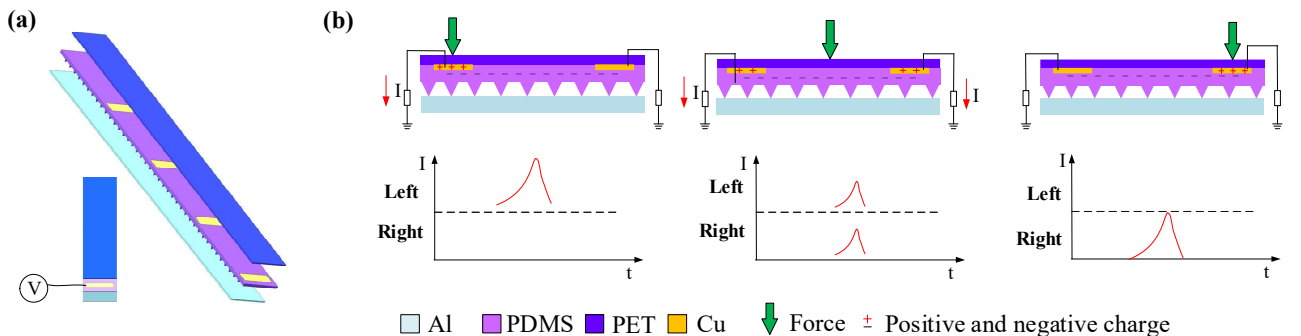


Fig.3 Structure design of TENG-based tactile sensor. (a) Integration process of the sensor. (b) Basic working principle of the TENG-based tactile sensor and the method to detect the contacting position.

of friction becomes larger, the amount of charge and the rate of charge generation at the two poles increase, so a gradually increasing potential will be generated, and the oscilloscope will display a correspondingly increased current. When the external force is released, the deformation of two poles would disappear. As two surfaces are separating away, the potential difference between the two poles decreases. Thus, positive charges of Cu layer induced by negative charges migrate to the ground so as to balance the static charge. Meanwhile, as the distance between the two poles increases, the rate of motion of the induced electrons decreases, resulting in a gradual decrease in the detected current (can be displayed on the oscilloscope).

The position sensing method for point-to-point contact is that as the silicone rubber featuring good electric negativity its surface is always negative charged. Thus during the contact to object with positive electrons, the electric balance between the electrode and the silicone rubber will be broken. Therefore, there will a potential difference and cause the electrons flow from the ground to the Cu electrode. As illustrated in Fig.3b, two electrodes have been used to display the position detection mechanism. When the object contacts near the left electrodes,

There will be a signal in the left electrode and the right electrode has no output vice versa. When the object contacts in the middle position of these two electrodes, due to the electrostatic induction, the similar output will be detected in both two electrodes and the signal is smaller than pressing the electrode directly. Herein, by comparing the signals' ratios in different electrodes, the contacting position can be sensed in the T-TENG sensor. Besides, for improving the precision, the signal ratio may expand compared to 1:1 and the electrode number can be increased.

III. MODELLING AND VERIFICATION

A. Analysis on Shape Perception Mechanism

The soft finger is actuated by the moment generated by the bellows expansion. Since it is difficult to accurately analyze the expansion-bending model of the flexible finger theoretically, the model analysis is based on the following assumptions: 1) During the expansion process, the single air cavity shape of the bellows is shown in the Fig.4a, where the y - z plane is circular and the x - y plane is oval. 2) The contact between two adjacent bellows air cavities is shown in the Fig.4b, where the contact area is the shadow shape (dark area), similar to an oval. 3) In the process of extrusion contact, the bending angle θ_1 of each air cavities is the same, as shown in Fig.4c. In order to simplify the theoretical calculation, the simply supported beam model is introduced to calculate the bending curve of the flexible fingers, as shown in Fig.4c, which is fixed at one end and free at the other hand.

We established the bending model, the contact force F is along with the direction of the line connecting the two centers of the circle. According to the static moment balance without external load, the following equation can be obtained:

$$PAr = -\frac{\theta EI}{l} \quad (1)$$

Where "-" indicates that the bending direction is negative

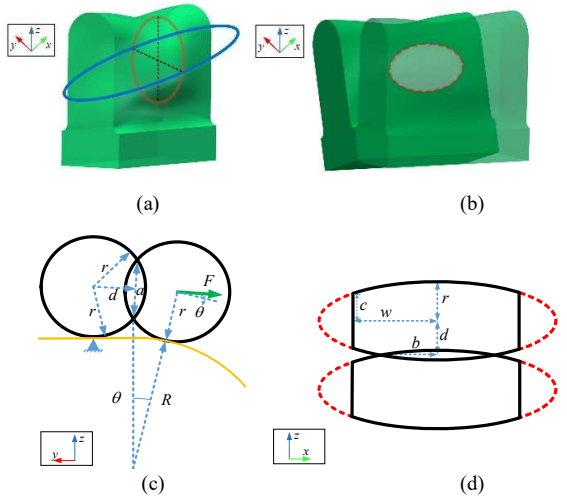


Fig. 4 Inflation model schematics of the soft finger. (a) Single air cavity. (b) Two air cavities interaction. (c) Analysis schematics of extrusion contact of two air cavity model lies in the y - z plane. (d) Analysis schematics of extrusion contact of two air cavity model lies in the x - z plane.

to z -axis. P is the air pressure. A is the contact area of the adjacent air cavity. r is the radius of the cross-section circle on y - z plane; θ is the rotation angle of the free end when subjected to a contact stress, whose value is equal to θ_1 solved by geometric calculation. E is the elasticity modulus of TPU, similar to that of nylon and rubber. I is the moment of inertia, a function of the dimensions. l is the distance from the fixed end to the moment point, and is the length of the projection of the tangent point between the two circles and the yellow line on the x - y plane in Fig.4c. Furthermore, l can be calculated as

$$l = 2d - r \sin \theta_1 \quad (2)$$

In our assumption 1, the contact area A is defined as an ellipse on x - z plane, thus, from the elliptic area formula, we have the following equation:

$$A = \pi ab \quad (3)$$

Where a and b are the short and long axes of the ellipse, respectively. From r and d , the parameter a of the ellipse can be described as

$$a = 2\sqrt{r^2 - d^2} \quad (4)$$

From the equation of the ellipse, b can be obtained as

$$b = w\sqrt{1 - \frac{d^2}{r^2}} \quad (5)$$

From the Fig.4c, we can approximately calculate that

$$d = (R + r) \sin \theta_1 \quad (6)$$

In our design, the length L of two tangent points can be simply settled. So another expression for d is

$$d = L - R\theta_1, \quad \theta_1 \text{ is radian} \quad (7)$$

Finally, due to θ_1 is a small angle, we can equate it to $\sin \theta_1$,

substituting the equation (2)-(7) into (1), the relationship between air pressure P and bending angle θ_1 of single air cavity can be described as

$$P\pi w^2 \frac{4r^2 - (L+r\theta_1)^2}{4(r^2 - c^2)} \sqrt{4r^2 - (L+\theta_1)^2} - \frac{EI}{L} = 0 \quad (8)$$

In the above equations, r can be calculated through the constant circumference of the cross-section circle on the x - y plane. L , w can be calculated with the design parameters, and E can be given according to the material properties. In the bending process, due to the hyperelastic property of TPU, deformation mainly occurs on the bottom of the finger (Fig.5a, blue line). Thus, force is generated to prevent the bending of finger when injected the high-pressure air, while strengthen the stability in grasping and holding an object. To facilitate the calculation, it is desirable to simplify the model displayed in Fig.5b. Based on the basic parameters and simple cantilever beam model, the inertia moment I of each bending unit can be computed as following equation:

$$I = \frac{Be_1^3 - b_1(h_1 - d_1)^3 + 2a_1e_2^3}{3} \quad (9)$$

Where $e_1 = \frac{2ah_1^2 + b_1d_1^2}{4ah_1 + 2b_1d_1}$, $e_2 = \frac{a(h_1 - e_1)^3}{3}$, represents the distance from the centre of mass to the corresponding edge, respectively.

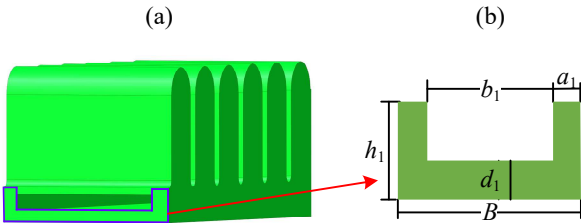


Fig.5 Sectional view. (a) Minimum section to resists the bending of finger. (b) The diameters of the magnified size diagram.

The bending deformation analysis of single soft finger has been completed. To realize the shape perception, we need to design a device to assemble the proposed finger. The placement of fingers would play a key role in the size of the objects that can be grasped and held. To verify the compliance and clarify the shape perception mechanism of our soft finger, the three-fingers type is adapted, of which the fingers are evenly distributed at 120° . Moreover, it is desirable to install the fingers with an angle α to the base. To ensure the reliable grasping and holding, the grasping device is suitable, as shown in Fig.6a. Obviously, the triangular structure increases the grasping stability, which is beneficial to apply the same magnitude pressure on each finger. Furthermore, the diameters of the device would determine the size, of which the grasper can manipulate the objects. Without connecting the high-pressure air, the gripper can manipulate objects with the radius from R_{\min} to R_{\max} . According to the dimensions in the Fig.6b, the minimum radius R_{\min} is as following:

$$R_{\min} = r_1 = \cot \frac{\alpha}{2} \quad (10)$$

In addition, to guarantee that the deformed fingers wrap around the surface of objects so as to improve the grip performance, the length of \overline{ef} should be longer than arc ed , illustrated in Fig.6d. There will be an inequality that

$$R_{\max} = R_1 < (m + n / 2 \cos \alpha) / (\frac{\pi}{2} - \alpha + \tan \alpha) \quad (11)$$

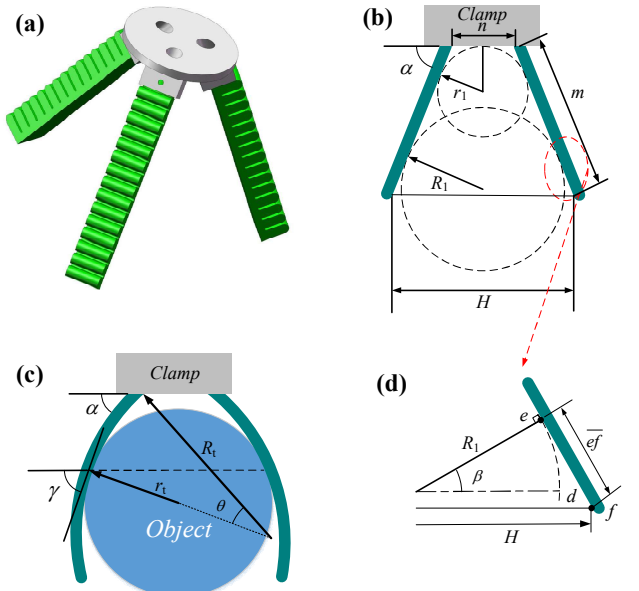


Fig.6 The size analysis of the object by soft fingers grasping device. (a) Diagram of the gripper integrated with fingers. (b) The largest gripping volume without air source. (c) The various size of object held by grasping device. (d) Magnified diagram.

The fundamental advantage of this gripper is the characteristic of adaption to contact between the fingers and objects. Applying the air pressure to the air cavity, fingers would naturally bend and contact with objects, causing the T-TENG sensor to generate a signal. Combining the position of signal and air pressure displayed on the barometer, the size can be simply calculated. As shown in Fig.6c, assume that contact occurs in a certain point of fingers, based on the above analysis and previous assumption 3, we will acquire the bending angle $\theta_i = i \times \theta$ of the contact point, which is same as arc angle between the base and the point. Correspondingly, the tangent line of that point will be an angle $\gamma = \alpha + \theta_i$ to the base. According to the principle of equal curvature arc, the radius r_t of object can be derived as follows

$$r_t = 2R_t \cot \frac{\theta_i}{2} \quad (12)$$

Where $R_t = \left| \frac{ds}{d\theta} \right| = \left| \frac{1}{\tan \theta_i} \right|$, is the radius of the equal curvature circle.

We calculate the angle of the adjacent finger bending when pressure was generated, and obtained the static bending angle under different pressure. Then, we can acquire that the angle of

the i th air cavity is $i \times \theta_1$. According to the above analysis, if the T-TENG sensor detects a signal, we would know the position and size of the grasped object based on air pressure.

B. Characteristics Tests of T-TENG

Based on TENG technology, T-TENG is quite like a simplified e-skin. This sensor based on TENG technology is able to sense the contacting area with low cost and high sensitivity. To recognize the size of the object, the position perception method has been introduced in section II. Here, we identified to possibility of the T-TENG sensor. In T-TENG, there are four electrodes. Here, we tested the four short electrodes for point-to-point contact as this is the most common way and the other test will be implemented in our future work. As depicted in Fig.7a, these four electrodes marked E1 to E4 from the left side is disturbed in the equal distance and the ideal output is listed in the left side.

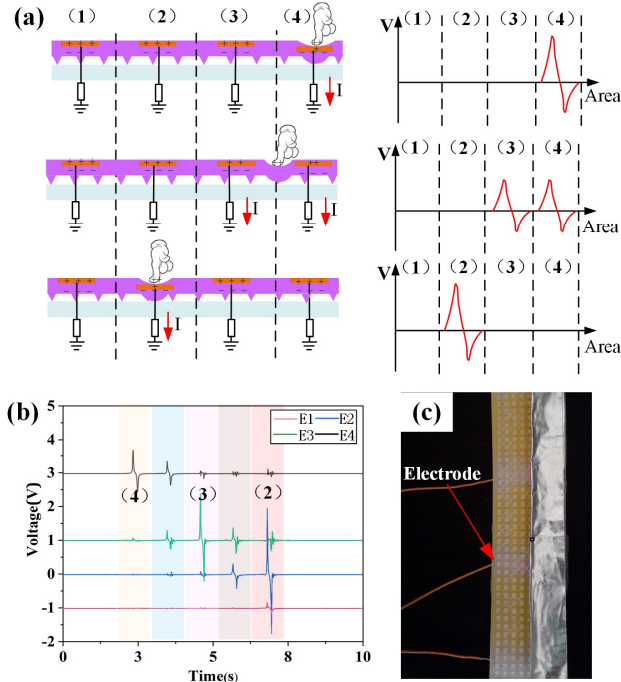


Fig.7 The T-TENG test. (a) The ideal output of the four electrodes. (b) The press test of T-TENG from E4 to E2. (c) The T-TENG device.

We tested the T-TENG with nitrile glove, which always has positive charge on its surface after contact with other material. In the test, we pressed both the electrodes and the middle of the two electrodes. The open circuit output was shown in Fig.7b. From the figure, we can find that the output in the different electrodes is changed. The reason is that it is hard to remain the same force and separated time for the human finger, which will affect the output of the TENG. However, this phenomenon will not affect the detection, if we compare the output voltage in different electrodes. The Fig.5b identifies that when we press the E2, E3 or E4, the corresponding electrode outputs apparent higher voltages than the others. As the contacting point changed to the middle of the electrodes like E3 and E4, the output in both electrodes is similar. Hence, based on the tests, the output

changes as the position varies and it is easy to recognize the contacting position.

C. Simple Tests on Shape Perception

For evaluating the performance of grasping and shape perception, we have carried out the tests on grasping objects of different sizes. The soft gripper integrated with T-TENG sensor is installed on a robot. Due to triangular structure of clamp, our experiment is mainly about symmetrical circular objects with regular shapes. After connecting to the air source, the pressure inside the cavity is displayed on the barometer at the current time, driving the fingers to bend and deform to contact the object. Meanwhile, the oscilloscope detects the output voltage on the sensor in real time.

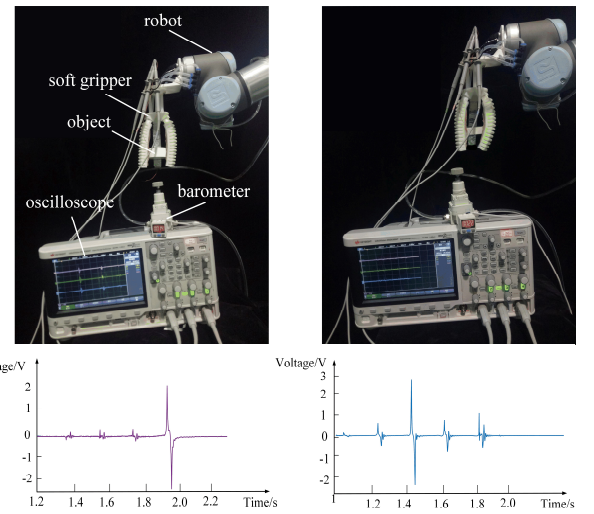


Fig.8 testing on various size objects. (a) Grasping test. (b) Waveform on the oscilloscope

Here, two different radius are tested, as shown in Fig.8a (small in the left and large in the right). To achieve the best state of tactile sensor detection performance, the object is placed in the position, where it will contact the sensor, and do not remove the external force until the soft fingers bend to support. Because it is difficult to ensure the sensor can contact with the object at the same time, the time and shape of the waveform generated at the three channels of the oscilloscope are different. In order to approach to the reality, we choose the waveform that occurs at last contact between object and soft fingers as the starting point of signal as shown in Fig.8b. Therefore, it is feasible to acquire position information by tactile sensor. The method that we can judge the shape of an object according to the given pressure and the position of the signal is effective.

IV. CONCLUSION

In this work, we presented the design and fabrication of a soft gripper that can roughly perceive the shape of the various objects, based on the soft finger and T-TENG sensor. The soft finger featured soft actuator, structure similar to bellows and integrated sensors. By 3D printing, a novel soft finger with complex inner geometry is manufactured directly combined with excellent features of TPU. To establish the grasping mechanisms theoretically, the fundamental analysis on bending

properties of the proposed fingers is described. The soft gripper has also been designed to show the working principle when manipulating the objects. The TENG-based tactile sensor of our work plays a significant role in assistant passive robot perception of shape, made up of Al and PDMS with different electrical properties. After the finger integrated with contact sensor inspired from TENG, we can acquire the information of the bending deformation and the contacting position, based on the above-mentioned method. Combining the signal with the calculation methods based on equal curvature hypothesis, the scale of the object can be obtained.

For verifying the sensing method, tactile sensor has been tested, which shows the output can be detected by the oscilloscope applying the pressure. Experiments have also been conducted to characterize the accuracy in grasping sundry size. Thus, the working mechanisms have also been verified. The soft gripper with shape and force based on Triboelectric Nanogenerator has great potential for dexterous hand application, we will work on the sensitivity of T-TENG and mechanical performance of soft finger in the future research to improve the accuracy.

REFERENCES

- [1] L. Li, T. Jin, Y. Tian, F. Yang, and F. Xi, "Design and Analysis of a Square-Shaped Continuum Robot with Better Grasping Ability," *IEEE Access*, vol. 7, pp. 57151–57162, 2019.
- [2] Rus and M. T. Tolley, "Design, fabrication and control of soft robots," *Nature*, vol. 521, no. 7553, pp. 467–475, 2015.
- [3] Y. Tian, M. Luan, X. Gao, W. Wang, and L. Li, "Kinematic analysis of continuum robot consisted of driven flexible rods," *Math. Probl. Eng.*, vol. 2016, 2016.
- [4] R. J. Webster and B. A. Jones, "Design and kinematic modeling of constant curvature continuum robots: A review," *Int. J. Rob. Res.*, vol. 29, no. 13, pp. 1661–1683, 2010.
- [5] T. G. Thuruthel, Y. Ansari, E. Falotico, and C. Laschi, "Control Strategies for Soft Robotic Manipulators : A Survey," vol. 5, no. 2, 2018.
- [6] Cai Jianguo*, Zhang Qian, Feng Jian, Xu Yixiang. Modeling and Kinematic Path Selection of Retractable Kirigami Roof Structures, Computer-Aided Civil and Infrastructure Engineering, 2019, 34(4): 352-363..
- [7] F. Renda et al., "Dynamic Model of a Multibending Soft Robot Arm Driven by Cables," *IEEE Trans. Robot.*, vol. 30, no. 5, pp. 1109–1122, 2014.
- [8] T. G. Thuruthel, E. Falotico, F. Renda, and C. Laschi, "Learning dynamic models for open loop predictive control of soft robotic manipulators Learning dynamic models for open loop predictive control of soft robotic manipulators," *Bioinspir. Biomim.*, 2017.
- [9] J. M. Croom, D. C. Rucker, J. M. Romano, and R. J. Webster, "Visual sensing of continuum robot shape using self-organizing maps," *Proc. - IEEE Int. Conf. Robot. Autom.*, pp. 4591–4596, 2010.
- [10] Z. Chen, Y. Shen, N. Xi, and X. Tan, "Integrated sensing for ionic polymer – metal composite actuators using PVDF thin films," vol. 16, 2007.
- [11] S. Song, Z. Li, M. Q. Meng, and H. Yu, "Real-Time Shape Estimation for Wire-Driven Flexible Robots With Multiple Bending Sections Based on Quadratic Bézier Curves," *IEEE Sens. J.*, vol. 15, no. 11, pp. 6326–6334, 2015.
- [12] H. Zhao, K. O. Brien, S. Li, and R. F. Shepherd, "Optoelectronically innervated soft prosthetic hand via stretchable optical waveguides," vol. 7529, no. December, pp. 1–10, 2016.
- [13] F. Fan, Z. Tian, and Z. Lin, "Flexible triboelectric generator !," *Nano Energy*, vol. 1, no. 2, pp. 328–334, 2012.
- [14] L. Shi et al., "Carbon electrodes enable flat surface PDMS and PA6 triboelectric nanogenerators to achieve significantly enhanced triboelectric performance," *Nano Energy*, vol. 55, no. November 2018, pp. 548–557, 2019.
- [15] Zhang Q, Dong Y, Peng Y, et al. "Asymmetric Bouc-Wen hysteresis modeling and inverse compensation for piezoelectric actuator via a genetic algorithm-based particle swarm optimization identification algorithm." *Journal of Intelligent Material Systems and Structures*, 2019, 30(8): 1263-1275.
- [16] T. He et al., "Beyond energy harvesting - multi-functional triboelectric nanosensors on a textile," *Nano Energy*, vol. 57, no. November 2018, pp. 338–352, 2019.
- [17] H. Li et al., "3D printed flexible triboelectric nanogenerator with viscoelastic inks for mechanical energy harvesting," *Nano Energy*, vol. 58, no. January, pp. 447–454, 2019.
- [18] T. Chen et al., "Triboelectric Self-Powered Wearable Flexible Patch as 3D Motion Control Interface for Robotic Manipulator," 2018.
- [19] X. Pu et al., "Rotation sensing and gesture control of a robot joint via triboelectric quantization sensor," *Nano Energy*, vol. 54, no. September, pp. 453–460, 2018.
- [20] Q. Shi and C. Lee, "Self-Powered Bio-Inspired Spider-Net-Coding Interface Using Single-Electrode Triboelectric Nanogenerator," *Adv. Sci.*, vol. 1900617, p. 1900617, 2019
- [21] Y. Hao et al., "A Soft Bionic Gripper with Variable Effective Length," vol. 15, pp. 220–235, 2018.
- [22] Y. Jiang, D. Chen, J. Que, Z. Liu, Z. Wang, and Y. Xu, "Soft robotic glove for hand rehabilitation based on a novel fabrication method," *2017 IEEE Int. Conf. Robot. Biomimetics, ROBIO 2017*, vol. 2018-Janua, pp. 1–6, 2018.
- [23] Cai Jianguo, Yang Ruigo, Wang Xinyu, Feng Jian. "Effect of Initial Imperfections of Struts on the Mechanical Behavior of Tensegrity Structures, Composite Structures," 2019, 207: 871–876
- [24] Tao Chen, Mingyue Zhao, Qiongfeng Shi, Zhan Yang, Huicong Liu, Lining Sun, Jianyong Ouyang, and Chengkuo Lee, "ovel Augmented Reality Interface Using A Self-Powered Triboelectric Based Virtual Reality 3D-Control Sensor," *Nano Energy*, 2018, 51, 162-172.